Magneto-tunnelling in double-barrier structures: the B perpendicular to J configuration

1992 J. Phys.: Condens. Matter 4 4125

(http://iopscience.iop.org/0953-8984/4/16/013)

J. Phys.: Condens. Matter 4 (1992) 4125–4134. Printed in the UK

Magneto-tunnelling in double-barrier structures: the $B \perp J$ configuration

H J M F Noteborn†, G H M van Tartwijk†§ and D Lenstra†‡
† Eindhoven University of Technology, Department of Physics, PO Box 513, 5600 MB Eindhoven, The Netherlands
‡ University of Leiden, Huygens Laboratory, Leiden, The Netherlands

Received 4 July 1991, in final form 30 December 1991

Abstract. The peak in the current–voltage (I–V) characteristic of a double-barrier resonant-tunnelling structure is broadened and lowered by the application of a magnetic field parallel to the layers. The broadening of the peak is roughly linear in the field. The lowering is completed at a field strength termed the quenching field. Both effects are described within a model of coherent tunnelling in a self-consistent potential. The calculated I–V curves agree well with experimental data.

1. Introduction

The double-barrier resonant-tunnelling (DBRT) structure is a well-known example of the novel devices based on the vertical transport mechanism. Its ability to carry current is based on the existence of a resonant state due to the quantum well between the two barriers. This state can be accessible to electrons in the Fermi sea of the reservoirs, formed by the doped regions that sandwich the DBRT structure. If we assume the tunnelling to be coherent, accessibility amounts to the demand that the energy of the resonant state is in the Fermi window of the reservoir. Since the resonance energy with respect to the reservoir is tunable by applying a voltage difference across the structure, there is always an interval of applied voltages where a current is possible. This vertical transport mechanism is essentially one-dimensional. The lateral dimensions only come into play in determining the density of states.

When we apply a magnetic field to a DBRT structure, perpendicular to the growth axis and parallel to the barrier layers, some basic aspects of the above picture are changed. The tunnelling is no longer dependent on the transverse motion alone. Accessibility of the resonant state is determined by the exchange of momentum between the transverse and lateral directions effected by the magnetic field. This leads to a smaller current density at voltages where, in the zero-field case, current was possible since some of the formerly resonant electrons are now filtered out on the basis of their lateral motion. At voltages where, in the zero-field case, no current was possible, however, there will now be some current density found since the magnetic field opens up the resonant channel for certain lateral momenta. In fact, the application of a perpendicular

§ Present address: Vrije Universiteit, Natuurkundig Laboratorium, Amsterdam, The Netherlands.

0953-8984/92/164125 + 10 $04.50

field has made the tunnelling into an essentially two-dimensional problem. In comparison with the zero-field case, the resulting current peak is broadened and lowered.

The implications of the magnetic field can also be described in another way. Let us introduce the difference between resonant states that are extended in both reservoirs (and which we will call 'extended' states), and resonant states that are evanescent in one of the two reservoirs (and which we will call 'semi-extended' states). The extended resonant states contribute to both the charge density in the well and the current density through the structure, whereas the semi-extended resonant states contribute only to the charge density in the well. In the zero-field case this distinction is not needed since all resonant states are extended. The perpendicular field, however, introduces the transformation of extended states into semi-extended ones, and the larger the applied field strength, the more complete is this transformation. At a certain field strength, all electrons are forced into semi-extended states, and hence the current will be zero, irrespective of applied voltage. This effect of the magnetic field can be called a quenching of the current, and the field strength above which this takes place is named the quenching field.

Experimental evidence for these effects of the transverse magnetic field was presented by Guéret *et al* [1], Rossel *et al* [2] and Ben Amor *et al* [3, 4], who reported a broadening and lowering of the current peak. Some theoretical work along semi-classical lines was done by Eaves and coworkers [5–7], whose distinction between 'traversing' and 'skipping' orbits parallels our extended/semi-extended states. A quantum-mechanical approach was undertaken by Ancilotto [8], considering a somewhat different structure (showing less interesting properties). We only mention here the work of Platero *et al* [9] which constitutes a totally different approach.

In this paper, a quantum-mechanical description of coherent resonant tunnelling in the presence of a perpendicular magnetic field is presented. Starting from the Schrödinger equation (section 2), we derive expressions for the voltage interval where resonant charge build-up takes place, and for the voltage interval where resonant current is found (section 3). In section 4, numerical results are presented for GaAs/AlGaAs-based structures. Finally we will compare our results with both experimental and theoretical studies (section 5).

2. Schrödinger equation with magnetic field

The usual way to introduce a magnetic field $\boldsymbol{B}$ into the Schrödinger equation is via the substitution $(\hbar/\mathrm{i})\nabla \rightarrow (\hbar/\mathrm{i})\nabla + e\boldsymbol{A}$, where $\boldsymbol{A}$ is the vector potential, related to $\boldsymbol{B}$ via $\boldsymbol{B} = \nabla \times \boldsymbol{A}$. Let us choose $\boldsymbol{A}$ to be defined by:

$$\boldsymbol{A} = \begin{cases} (0, \quad 0, \quad 0) & z < 0 \\ (0, -Bz, \ 0) & 0 < z < L \\ (0, -BL, 0) & L < z \end{cases} \tag{1}$$

yielding a magnetic field in the x-direction of strength B if $0 < z < L$, and of zero strength outside this interval. Equation (1) implies a Coulomb gauge $\nabla \cdot \boldsymbol{A} = 0$ and a coupling of the magnetic field to the y-component of the momentum only. This choice for a magnetic field confined to the interval $0 < z < L$ agrees with the usual and accepted approach in device modelling [1, 5, 6]. It is also supported by the physical processes in the reservoirs, where the bulk scattering of carriers will cause effective broadening of the Landau levels

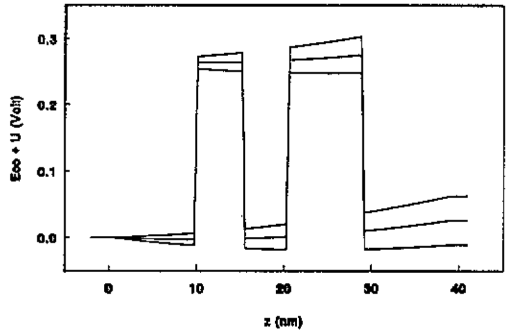

Figure 1. Potential energy of electrons in the DBRT structure as a function of position z, drawn for three different values of k_y. The applied voltage $V_a = 0$ V, the magnetic field strength $B = 5$ T.

and, eventually a density of states approaching the zero-field behaviour [5]. The value of L is thus expected to be related to the mean free path of electrons in the reservoir. In this paper, however, we will treat L as an extra parameter. The possibilities of determining L by experiment will be discussed in section 5. The choice (1) has the advantage of enabling a transfer matrix approach, with plane wave solutions in the reservoirs, which are easy to interpret in terms of current density.

We insert the vector potential of (1) into the Schrödinger equation:

$$(1/2m)\left((\hbar/i)\nabla + eA(z)\right)^2\Psi(r) + E_{co}(z)\Psi(r) = E\Psi(r) \tag{2}$$

where $\Psi(r)$ describes the electrons in the conduction band, m is the effective mass of this band and $E_{co}(z)$ is the band minimum. The z-axis is taken along the growth direction. In general, the materials of the barriers and the well will differ in both effective mass and band gap. We will, however, take into account only the latter difference, and write $E_{co}(z)$, assuming m independent of z. In the reservoir situated at $z < 0$ we have both $E_{co}(z) = 0$ and $A(z) = \mathbf{0}$, so that the solutions of (2) are plane waves

$$\exp(ik_x x)\exp(ik_y y)\left[A\exp(ik_z z) + B\exp(-ik_z z)\right]$$

at energy $E = (\hbar^2/2m)(k_x^2 + k_y^2 + k_z^2)$. Since the Hamiltonian in (2) is invariant under translation in the lateral directions, the wave-number components k_x and k_y (contrary to k_z) are constants of motion. Substituting for $\Psi(r)$ the factorization $\exp(ik_x x)$ exp-$(ik_y y)F(z)$, we have (2) to read:

$$\begin{aligned} -(\hbar^2/2m)(d^2/dz^2)F(z) + E_{co}(z)F(z) + U(z;k_y,B)F(z) \\ = \left(E - (\hbar^2/2m)(k_x^2 + k_y^2)\right)F(z) = (\hbar^2 k_z^2/2m)F(z) \end{aligned} \tag{3}$$

where $U(z;k_y,B)$ is a potential energy term introduced by the magnetic field, that is quadratic in z and B and linear in k_y (see figure 1):

$$U(z;k_y,B) = \begin{cases} 0 & z < 0 \\ (e^2B^2/2m)z(z - 2\hbar k_y/eB) & 0 < z < L \\ (e^2B^2/2m)L(L - 2\hbar k_y/eB) & L < z. \end{cases} \tag{4}$$

In the absence of $E_{co}(z)$ in (3), we would find for $0 < z < L$ that $F(z) = A'D_\nu(\zeta) + B'D_{-\nu-1}(i\zeta)$, where $D_\nu(\zeta)$ is the parabolic cylinder function, $\nu = \hbar(k_y^2 + k_z^2)/2eB - \frac{1}{2}$, and $\zeta = \sqrt{(2eB/\hbar)}\,(z - \hbar k_y/eB)$ [10]. A restriction to a non-negative integer ν would give the well-known Landau levels. Usually, it is the requirement for normalization on the z-interval $(-\infty, +\infty)$ that leads to this quantization of energy [10]. However, since the quadratic potential in (4) applies only to $0 < z < L$, we have no Landau quantization in this tunnelling problem, and hence no Landau levels. Instead, we calculate the transmission and reflection coefficients for incoming plane waves labelled with k_z and scattered by a k_y-dependent potential. The eigenfunctions $F(z; k_y, k_z)$ now depend on the lateral momentum, in contrast to the zero-field case, although the eigenvalues still depend on k_z only. This means that (3) constitutes a tunnelling problem where we have to treat every combination (k_y, k_z) separately. The resulting transmission and reflection coefficients will be functions of both transverse and lateral momentum.

3. Voltage interval of resonant current

To find the voltage interval where resonant charge built-up or current takes place we make use of the fact that the resonant energy with respect to the band minimum in the well is almost independent of the exact potential structure. Hence, we determine this energy E_0 in the unbiased zero-field situation and treat it as a constant. In this section, we also assume a constant electric field in the structure, neglecting the effect of the charge build-up in the well on the band bending. The potential energy in the well then equals $-\alpha e V_a$, where V_a is the applied voltage and $0 < \alpha < 1$ depends on the structure parameters. For identical barriers, $\alpha = 1/2$. Let us first consider the zero magnetic field case. For the resonance energy to be in the Fermi window of the reservoir means: $0 < E_0 - \alpha e V_a < E_F$, hence the voltage interval for resonant current and charge build-up is: $(E_0 - E_F)/e\alpha < V_a < E_0/e\alpha$.

In the case of a magnetic field, the potential term $U(z; k_y, B)$ of (4) should be included, making these relations dependent on k_y. Also, at fixed k_y, the possible energies related to the transverse momentum are limited to $0 < \hbar^2 k_z^2/2m < E_F - \hbar^2 k_y^2/2m$, i.e. the window for the resonance energy is reduced. The condition for resonant charge build-up therefore becomes:

$$0 < E_0 - \alpha e V_a + U(z_w; k_y, B) < E_F - \hbar^2 k_y^2/2m \tag{5}$$

where z_w is the position of the well. This can again be translated into a corresponding voltage interval:

$$\begin{aligned} &V_{a1}(k_y, B) < V_a < V_{a2}(k_y, B) \\ &V_{a1}(k_y, B) \equiv (E_0 - E_F)/e\alpha + (\hbar k_y - eBz_w)^2/2me\alpha \\ &V_{a2}(k_y, B) \equiv E_0/e\alpha + eB^2 z_w^2/2m\alpha - \hbar k_y B z_w/m\alpha \end{aligned} \tag{6}$$

which is sketched in figure 2. For resonant current to flow, an additional condition with no zero-field analogue is to be introduced. The transverse momentum in the collector reservoir should be positive in order to enable an electron to contribute to the current. This yields:

$$E_0 - \alpha e V_a + U(z_w; k_z, B) > -eV_a + U(L; k_z, B) \tag{7}$$

which is trivial for $B = 0$. Translated in terms of V_a, (7) reads:

$$V_a > V_{a3}(k_y, B) \equiv [1/(1-\alpha)](-E_0/e + eB^2(L^2 - z_w^2)/2m - \hbar k_y B(L - z_w)/m) \tag{8}$$

(see figure 2). If an electron state with momentum k_y and resonant k_z satisfies (6) but

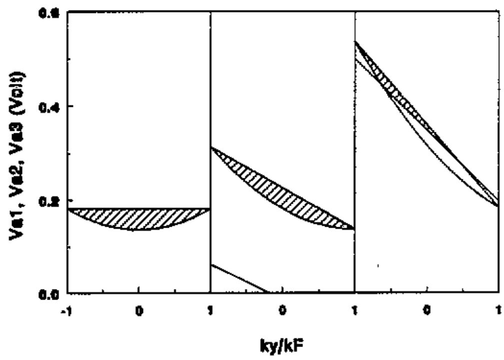

Figure 2. $V_{a1}(k_y)$, $V_{a2}(k_y)$ and $V_{a3}(k_y)$ for three different values of the magnetic field B. The states corresponding to points in the enclosed area contribute to the charge density in the well. The hatched area represents states that, in addition, contribute to the current through the structure.

not (8), it contributes to the charge density in the well only. This is a so-called 'semi-extended' state. If the electron state meets both conditions (6) and (8), it contributes to both the charge and the current density, and is called 'extended'.

The voltage interval that results from (6) depends on k_y. Thus, at a given applied voltage V_a, (6) will be met by only a fraction of all k_y-values. This implies a decrease in charge density, compared with the zero-field case. Using the fact that $\hbar^2 k_y^2/2m < E_F$, we can define voltage intervals where we have taken into account the contributions of all k_y. For the charge build-up this means that we have to find the minimum of $V_{a1}(k_y)$, denoted by $\bar{V}_{a1}$, and the maximum of $V_{a2}(k_y)$, denoted by $\bar{V}_{a2}$. The latter is equal to $V_{a2}(-k_F)$ for all field strengths, k_F being the Fermi wave-number. For $B < B_0 \equiv \hbar k_F/ez_w$, $\bar{V}_{a1} = V_{a1}(eBz_w/\hbar)$. For larger field strengths, it is $V_{a1}(+k_F)$. Hence, we find for the sum of all k_y-contributions that, in order for the charge in the well to be non-zero at V_a, V_a should satisfy:

$$\bar{V}_{a1}(B) < V_a < \bar{V}_{a2}(B)$$

$$\bar{V}_{a1}(B) = \begin{cases} V_{a1}(eBz_w/\hbar, B) = (E_0 - E_F)/e\alpha & B < B_0 \\ V_{a1}(+k_F, B) = E_0/e\alpha + ez_w^2 B(B - 2B_0)/2m\alpha & B > B_0 \end{cases} \tag{9}$$

$$\bar{V}_{a2}(B) = V_{a2}(-k_F, B) = E_0/e\,\alpha + ez_w^2 B(B + 2B_0)/2m\alpha.$$

These interval bounds as functions of B are shown in figure 3(a). From (9) we see that $\mathrm{d}\bar{V}_{a1}/\mathrm{d}B \geqslant 0$ and $\mathrm{d}\bar{V}_{a2}/\mathrm{d}B > 0$, hence both bounds are non-decreasing functions of B. Since the upper bound increases faster, the total voltage interval for charge build-up is broadened, see figure 3(b). For $B \geqslant B_0$ this broadening is linear in B: $\Delta\bar{V}_a \equiv \bar{V}_{a2} - \bar{V}_{a1} = ez_w^2 4BB_0/2m\alpha = (2\hbar k_F z_w/m\alpha)B$.

To find out whether the total voltage interval for resonant current is also broadened, we have to take into account the effect of (8) on the bounds. This is an easy but complicated matter, depending on α, z_w/L and E_F/E_0. Therefore, we will only give the results for the special case that $(z_w/L)^2 < \alpha < z_w/L$ and $E_F < E_0/(1 - 2\alpha L/z_w + \alpha L^2/z_w^2)$. Since, experimentally $\alpha \approx 1/2$, $z_w/L \approx 1/2$ and $E_0 \gg E_F$, this is the most relevant case. For small field strengths, we find the same bounds as in the charge build-

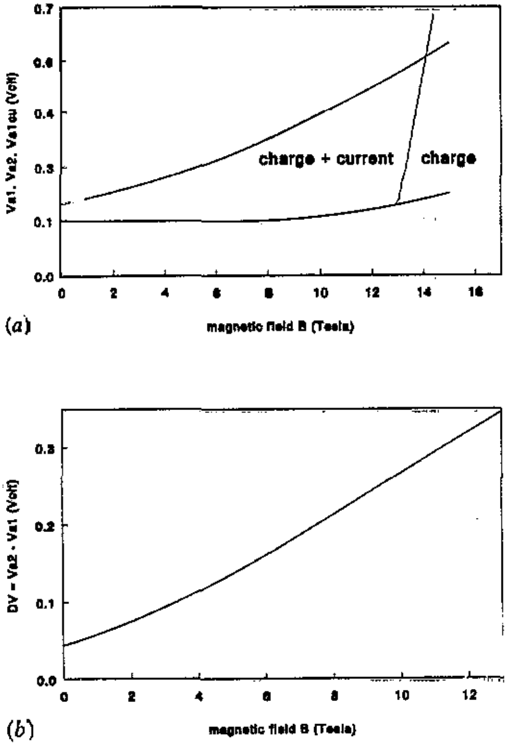

Figure 3. (*a*) $\bar{V}_{a1}(B)$ and $\bar{V}_{a2}(B)$, as well as $\bar{V}^{cu}_{a1}(B)$ and $\bar{V}^{cu}_{a2}(B)$. For V_a between $\bar{V}_{a1}(B)$ and $\bar{V}_{a2}(B)$ electrons can enter the well resonantly. For V_a between $\bar{V}^{cu}_{a1}(B)$ and $\bar{V}^{cu}_{a2}(B)$ they can leave the well at the collector side; (*b*) the width of the current peak $\Delta\bar{V}_a \equiv \bar{V}_{a2} - \bar{V}_{a1}$ as a function of the magnetic field strength B.

up situation, as expected. If, however, B exceeds a value V_-:

$$B_\pm = \pm\frac{\hbar k_F}{eL}\frac{z_w/L-\alpha}{\alpha-(z_w/L)^2} + \frac{1}{eL}\left[2mE_F\left(\frac{z_w/L-\alpha}{\alpha-(z_w/L)^2}\right)^2 + 2mE_0\frac{1}{\alpha-(z_w/L)^2}\right]^{1/2}$$

the lower bound is changed to:

$$\bar{V}^{cu}_{a1}(B) = [z_w/L-\alpha]^{-1}\left(-E_0/e + eB^2 z_w(L-z_w)/2m\right)$$

whereas the upperbound remains unchanged, $\bar{V}^{cu}_{a2}(B) = \bar{V}_{a2}(B)$. This new lower bound $\bar{V}^{cu}_{a1}(B)$ increases more rapidly than the upper bound, so that at $B = B_+$ the two bounds coincide and the voltage interval disappears completely. Therefore, we say that the current is 'quenched' at $B = B_+$ and we call this field strength B_+ the 'quenching field'. A particularly simple form for this quenching field is obtained in the limit $E_F/E_0 \to 0$, i.e. in the case of a small well width:

$$B_+ = (1/e)[2mE_0/z_w(L-z_w)]^{1/2}. \qquad (11)$$

The same expression is found for the special case that $\alpha = z_w/L$. Equation (11) allows a classical or geometric interpretation (see figure 4): a particle having a transverse momentum $p_z = (2mE_0)^{1/2}$ at $z = z_w$ will move along the curtate cycloid $y = \frac{1}{2}L(\sin\varphi - \varphi) - (\hbar k_F/eB_+)\varphi$, $z = \frac{1}{2}L(1-\cos\varphi)$ if $B = B_+$. The general expression, depending also on E_F and α, lacks such a transparent interpretation.

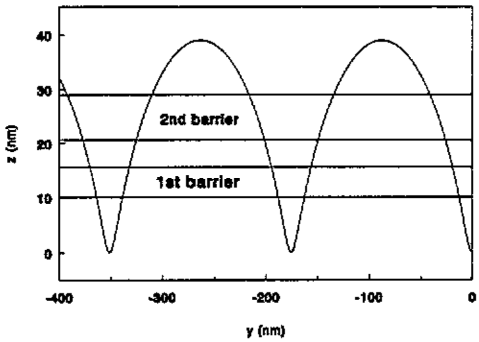

Figure 4. Classical trajectory of a particle in crossed electric and magnetic field to illustrate the quenching field B_+ of (11).

In this section, we have demonstrated the lowering and broadening of the current peak due to the application of a perpendicular magnetic field. We have assumed that the resonance energy can be treated as a constant, and that the transmission peak has negligible width. We have only considered resonant current and charge build-up, and have ignored all demands of self-consistency. The quenching field, following from this analysis, is a consequence of the transformation by the magnetic field of extended states into semi-extended ones. Expressions for this field, calculated for the zero-temperature case, provide an estimate for the length L over which the magnetic field is effective. In the next section, we present numerical calculations in which some of the above-mentioned restrictions are avoided.

4. Numerical results

To present I–V curves for structures in a perpendicular magnetic field, numerical calculations were done, assuming a GaAs/AlGaAs structure characterized by an effective mass of 0.067 times the free electron mass, and a band discontinuity of 0.44 eV. Barrier widths are 5.6 nm, the well is 5.0 nm wide. Details of the model can be found in [11]. Here, we only mention the adjustments to the magnetic field situation. The Schrödinger equation (3, 4) is quadratic in coordinate z. Its basic solutions can therefore be chosen to be parabolic cylinder functions [10]. However, to avoid the difficulties inherent in working with these special functions and to reduce computational time, we have approximated the potential in each of the five layers (emitter, barrier, well, barrier, collector) by its average value, thus obtaining plane waves at every position in the structure. This apparently drastic approximation turns out to have little effect on the I–V characteristics [12] while shortening calculations considerably. The length L over which the magnetic field is thought to be effective is taken to equal the structure length [5]. The effect of the charge density in the well on the band bending is taken into account self-consistently. The main difference with the zero-field calculations is that the summation over the lateral momenta can now not be done analytically, but necessitates an extra loop, enormously enlarging computational times.

In figure 5 a series of I–V curves is plotted for magnetic field strengths ranging from 5 T to 30 T. The lowering and broadening of the current peak, anticipated in the previous section, are confirmed by the self-consistent calculations. The quenching field is more easily illustrated by the I–B curves of figure 6. Here, the effect of the charge build-up on

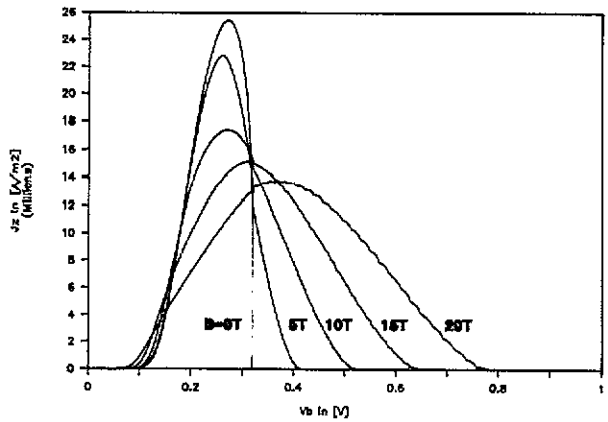

Figure 5. *I–V* curves for eight different values of the magnetic field strength *B*, resulting from self-consistent calculations. $T = 77$ K.

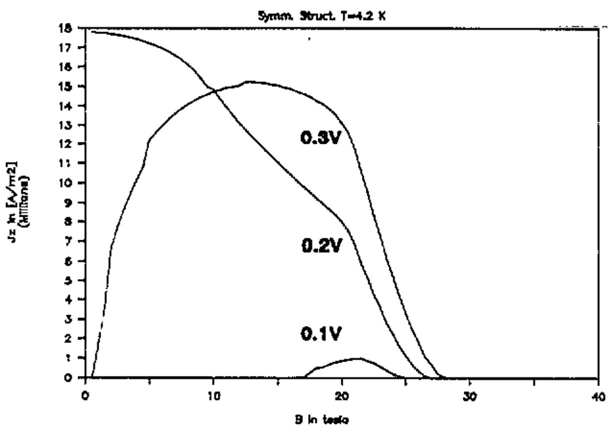

Figure 6. *I–B* curves for three values of the applied voltage V_a, resulting from self-consistent calculations. $T = 4.2$ K.

the band bending is seen in the small shift of the quenching field to the larger values for increasing applied voltage V_a. The value of the quenching field, around 30 T, may seem experimentally out of reach. However, these unrealistically large fields are the price we have to pay for the simplification of equalling L with the structure length, thus greatly underestimating L. Neglecting arguments of self-consistency, we may say that the quenching field is inversely proportional to L, so that a three times larger L leads to fields that are accessible to experiment.

5. Discussion

Good agreement with the experimental findings of Ben Amor and co-workers [3, 4] is found. Their I–V curves (figure 1 in [4]) agree well with the ones we present in figure 5. Also, the observed linear increase of the width of the current peak with B [1, 2, 4] is confirmed by our analysis. For $B_0 < B < B_-$ a linear relation holds for the voltage interval width and the magnetic field strength, corresponding to a slope that equals $2\hbar k_F z_w / m\alpha$. Taking $z_w/L = \alpha$, this agrees well with the results of [4]. For $B < B_0$ a quadratic increase is predicted by (9), whereas for $B > B_-$ a change from increase to decrease is expected. These two regions, however, are not covered by the experimental data. Because of a bad choice of structure parameters, Ancilotto does not find a substantial broadening of the current peak [8].

The decrease of the peak current with increasing magnetic field is found in all experiments [1, 4]. However, this decrease does not continue as expected in our model. In fact, the peak current reaches a minimum around 16 T for the AlInAs/GaInAs structure [4], and around 5 T for the GaAs/AlGaAs structure (see figure 9 in [1]). This is thought to be an indication that coherent tunnelling cannot be the whole story [2]. Sequential effects, or better inelastic scattering proceses, seem to be more important in GaAs/AlGaAs than in AlInAs/GaInAs.

As a consequence, the quenching field is not directly obtainable from experiments. It can only be extrapolated from the initial decrease of the peak current. However, the linear increase of the current width with magnetic field still provides a means of estimating the length L, over which B is to be taken into account [1]. In the GaAs/AlGaAs structure, L is found to be ~35 nm [1], corresponding to a quenching field of about 10 T. In the AlInAs/GaInAs sample, the quenching field is larger, owing to a much smaller effective length L (8.5 nm [4]).

The decrease of the turn-on voltage $\bar{V}_{a1}(B)$, reported in [4], is not expected from our analysis (see (9)), nor confirmed by the measurements of [1] or the analysis in [6]. However, the accuracy of the data supporting this result in [4] is probably such that they could also support Leadbeater's or our analysis. This minor point of difference does not affect the overall agreement.

The difference between extended and semi-extended states, introduced in section 3, is also met in Eaves *et al* [7]. There, the two types of state are associated with 'traversing' and 'skipping' orbits. The latter, interacting with the emitter barrier only, contribute to the density in the well. In a traversing state an electron is repeatedly reflected off both barriers. In the semi-classical picture, the important length scale is set by the well width. In the quantum mechanical picture, this role is played by the effective length L. Although a theory for L is missing, it is thought that L is related to the mean free path rather than to the well width. Hence, both pictures may not be totally identical.

From the derivation of (9), it is clear that the expressions for $\bar{V}_{a1}$ and $\bar{V}_{a2}$ depend on the applied dispersion relation for the conduction band, in our model a simply quadratic one. Inclusion of non-parabolicity or an energy-dependent effective mass, or—in the case of holes—band mixing, will yield different expressions for these quantities. Conversely, experimental determination of quantities like $\bar{V}_{a1}(B)$ and $\bar{V}_{a2}(B)$ provides a powerful method for investigating the dispersion curves [13].

Summarizing, we have presented a quantum-mechanical study of the effect of a transverse magnetic field on coherent resonant tunnelling. The calculated I–V curves agree well with experimental data. The quenching field, although experimentally obscured by incoherent processes, is still a valuable quantity, containing information about the resonance energy and the effective length L for the vector potential. The presented model provides a good description for structures in which coherent tunnelling is dominant.

Acknowledgments

We would like to thank H P Joosten for fruitful discussions. This work is part of the research programme of the Foundation for Fundamental Research on Matter (FOM), which is financially supported by the 'Nederlandse Organisatie voor Wetenschappelijk Onderzoek' (NWO).

References

[1] Guéret P, Rossel C, Marclay E and Meier H 1989 *J. Appl. Phys.* **66** 278
[2] Rossel C, Guéret P and Meier H P 1990 *J. Appl. Phys.* **67** 900
[3] Ben Amor S, Martin K P, Rascol J J L, Higgins R J, Torabi A, Harris H M and Summers C J 1988 *Appl. Phys. Lett.* **53** 2540
[4] Ben Amor S, Rascol J J L, Martin K P, Higgins R J, Potter R C and Hier H 1990 *Phys. Rev.* B **41** 7860
[5] Eaves L, Stevens K W H and Sheard F W 1988 *The Physics and Fabrication of Microstructures and Microdevices (Springer Series in Physics 13)* (Berlin: Springer) p 343
[6] Leadbeater M L, Eaves L, Simmonds P E, Toombs G A, Sheard F W, Claxton P A, Hill G and Pate M A 1988 *Solid State Electron.* **31** 707
[7] Eaves L, Alves E S, Henini M, Hughes O H, Leadbeater M L, Payling C A, Sheard F W, Toombs G A, Celeste A, Portal J C, Hill G and Pate M A 1989 *High Magnetic Fields in Semiconductor Physics II* ed G Landwehr (Heidelberg: Springer) 324
[8] Ancilotto F 1988 *J. Phys. C: Solid State Phys.* **21** 4657
[9] Platero G, Schulz P A, Brey L and Tejedor C 1990 *Surf. Sci.* **228** 291, and references therein
[10] See e.g.
Erdelyi A, Magnus W, Oberhettinger F and Tricomi F G 1953 *Higher Transcendental Functions* 2 (New York: McGraw-Hill) p 116
Merzbacher E 1961 *Quantum Mechanics* (New York: Wiley) p 70
Greiner W 1989 *Quantum Mechanics (Theoretical Physics 1)* (Berlin: Springer) p 114
[11] Joosten H P, Noteborn H J M F and Lenstra D 1990 *Thin Solid Films* **184** 199
Noteborn H J M F, Joosten H P and Lenstra D 1990 *Phys. Scr.* *T* **33** 219
Noteborn H J M F, van Tartwijk G H M, Joosten H P and Lenstra D 1991 *J. Phys.: Condens. Matter* **3** 4249
[12] See e.g.
Mendez E E 1987 *Physics and Applications of Quantum Wells and Superlattices* ed E E Mendez and K von Klitzing (New York: Plenum) 159
[13] Cury L A, Celeste A, Goutiers B, Ranz E, Portal J C, Sivco D L and Cho A Y 1990 *Superlatt. Microstruct.* **7** 415
Hayden R K, Maude D K, Eaves L, Valadares E C, Henini M, Sheard F W, Hughes O H, Portal J C and Cury L 1991 *Phys. Rev. Lett.* **66** 1749